LETTER

Coating Evaporated MAPI Thin Films with Organic Molecules: Improved Stability at High Temperature and Implementation in High-Efficiency Solar Cells

Francisco Palazon,*[†,§] Daniel Pérez-del-Rey,[§] Sergio Marras,[‡] Mirko Prato,[‡] Michele Sessolo,[§] Henk J. Bolink,[§] and Liberato Manna[†]

[†]Nanochemistry Department, and [‡]Materials Characterization Facility, Istituto Italiano di Tecnologia, Via Morego 30, 16163 Genova, Italy

[§]Instituto de Ciencia Molecular, ICMol, Universidad de Valencia, C/Catedrático J. Beltrán 2, 46980 Paterna, Spain

Ⓢ *Supporting Information*

ABSTRACT: Methylammonium lead iodide (MAPI) has proven to be an exceptional light-absorber for single-junction thin-film solar cells. Nonetheless, degradation induced by environmental agents (air, moisture, heat) limits the stability of this hybrid perovskite. Here, we demonstrate that coating evaporated MAPI thin films with different hydrophobic molecules leads to a significant improvement in their stability. We especially investigated the degradation of MAPI and the subsequent formation of PbI_2 at 150 °C by in situ XRD analysis and showed that this transformation is remarkably slowed down in films coated with trioctyl phosphine oxide and tridodecyl methylammonium iodide. This enhances the processability of such films, which is an important aspect for the fabrication of thin-film devices. Eventually, we demonstrate that such protected films can be implemented in single-junction n–i–p solar cells without any loss in the device efficiency.
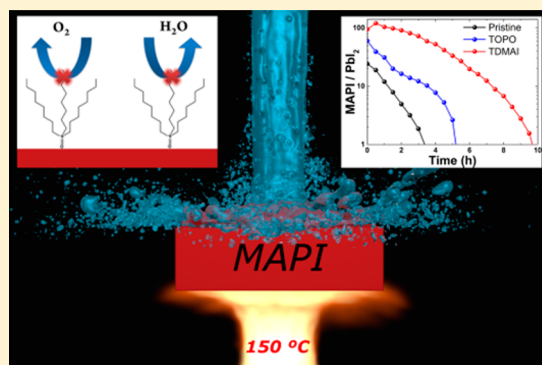
As widely reported in the past few years, methylammonium lead iodide ($CH_3NH_3PbI_3$; MAPI) is an excellent material for single-junction solar cells and other optoelectronic devices.[1–4] The outstanding performances of these devices can be linked to several photophysical properties of perovskites, such as their high absorption coefficient, narrow bandgap, and high charge diffusion lengths,[5,6] together with the ease of fabrication and low cost of precursors.[7] Nonetheless, the widespread use of MAPI is currently severely hindered by its well-known instability. Indeed, oxygen, water (moisture), and heat among other factors are known to lead to a fast degradation of MAPI thin films.[8,9] In order to mitigate this instability, one possible approach is to alter the material composition, as already demonstrated in many reports. These modifications include the partial substitution of I^- anions with Br^- anions,[10] the partial or total substitution of MA cations with other organic or inorganic monovalent cations such as formamidinium ($CH(NH_2)_2^+$; FA), cesium (Cs^+), or rubidium (Rb^+),[11–13] or the incorporation of 2D perovskites.[14–18] These substitutions can lead to rather complex formulations comprising up to seven different ions whose relative amounts

need to be well controlled.[19] Furthermore, bromide-based and 2D perovskites have a higher bandgap than their 3D iodide counterparts, which is not beneficial for photovoltaic (PV) applications.[14–18] Hence, it is critical to explore new ways of enhancing the stability of MAPI films without necessarily altering their overall composition. Because degradation often initiates at the surface of the films through its exposure to external species (e.g., moisture),[20] one possible strategy is to chemically modify the perovskite surface with different organic molecules. Yang et al.[21] showed that coating the surface of solution-processed MAPI thin films with different hydrophobic molecules leads to an increased stability in a high-moisture environment at room temperature. The same approach has recently been developed by Wang et al.,[22] while deQuilettes et al.[23] found that surface modification with Lewis base molecules leads to efficient passivation of the nonradiative surface trap states. Huang et al. also noticed an increase of initial efficiency

as well as stability in single-junction solar cells with a similar method.[24] A critical aspect to consider for the widespread implementation of MAPI in thin-film devices is its stability at high temperature (>100 °C). Although this may seem irrelevant for typical operation conditions, it is important to evaluate the stability at high temperature in view of the fabrication of optoelectronic devices. Indeed, the typical fabrication processes of thin-film devices require the deposition of several additional layers on top of the active (perovskite) film such as charge extracting layers, electrodes, or encapsulation materials. Depending on the process and the material, these further depositions may require temperatures well above 100 °C. In this Letter, we have coated vacuum-deposited MAPI thin films with trioctyl phosphine oxide (TOPO) and tridodecyl methylammonium iodide (TDMAI), adapting reported protocols by deQuilletes et al.[23] and Yang et al.,[21] respectively. We demonstrate in both cases the presence of ultrathin layers of TOPO and TDMAI through direct chemical characterization by X-ray photoelectron spectroscopy (XPS). Then, we show by in situ X-ray diffraction (XRD) that the so-coated films have a drastically enhanced stability in air at 150 °C. Eventually, we demonstrate that the presence of these layers is not incompatible with the good operation of PV devices. As a proof-of-principle, we fabricate single-junction solar cells with pristine and coated MAPI in n−i−p configurations that show promising efficiency and stability.[25]

MAPI thin films were prepared by dual-source vacuum deposition on glass substrates, as explained in the experimental section. Then, the films were coated either with TDMAI or TOPO. Adapting reported protocols,[21,23] TDMAI-coated samples were realized by fully immersing the MAPI thin films in a 25 mM solution in isopropanol, while the TOPO-coated samples were prepared by a single spin-coating step of a 25 mM TOPO solution in toluene (see the Supporting Information for more details).

Figure 1a shows wide XPS spectra of pristine and TDMAI-coated films. Although TDMAI does not have any distinctive
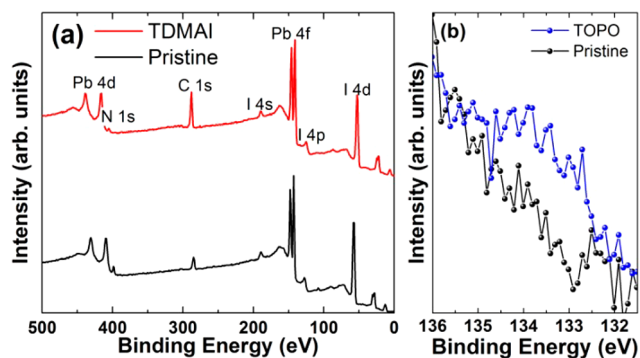
Figure 1. XPS characterization of pristine MAPI films as well as films coated with TDMAI and TOPO. (a) Wide scans of pristine and TDMAI samples and (b) narrow scans of the P 2p region of pristine and TOPO samples (see Figure S1 for XPS characterization of a sample with a thicker layer of TOPO).

chemical element other than the ones present already in the MAPI film, XPS reveals an increase in the carbon content of the film surface after functionalization (the C:Pb ratio increases by a factor of >3), which proves the attachment of TDMAI molecules to the surface. Figure 1b shows XPS narrow scans of the region corresponding to 2p orbitals from phosphorus (P

2p). The increase in signal is evident proof of the presence of TOPO (see Figure S1 for XPS characterization of a film coated with a 50 mM solution of TOPO). Yet, the signal remains very low, which is expected for a thin layer. This is important in order to allow charge tunneling with electron or hole transport layers in solar cells and, generally speaking, to allow the use of such coated films in optoelectronic devices. Next, the stability of pristine and coated films at 150 °C was evaluated by in situ XRD measurements (Figure 2). As mentioned before, thermal
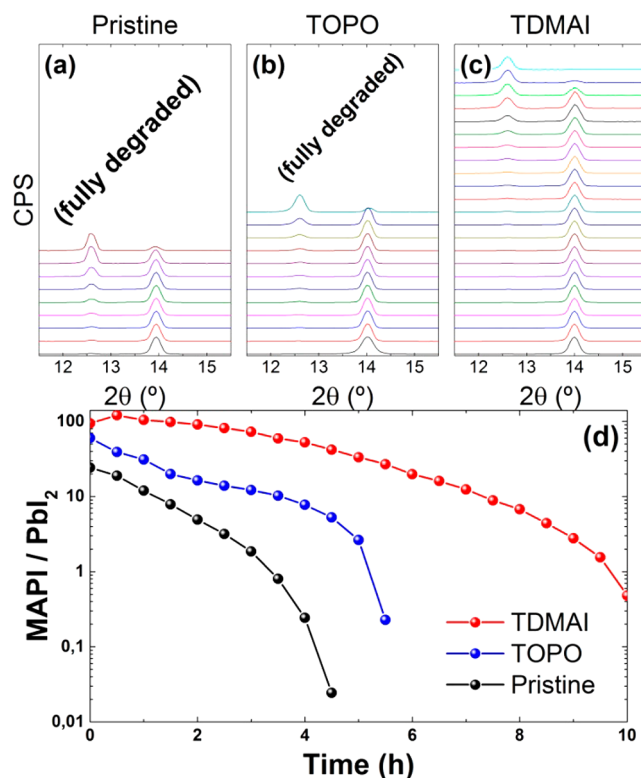
Figure 2. XRD characterization of sample degradation at 150 °C. (a−d) Diffractograms of pristine (a) and coated (b,c) films over time. Initial scan at the bottom, 30 min between each scan. (d) Intensity ratio between the main perovskite and PbI$_2$ peaks (2θ = 14.0 and 12.6°, respectively), computed from panels (a−c).

annealing above 100 °C is a common step in many thin-film fabrication procedures (atomic layer deposition, sputtering, etc.); hence, it is technologically relevant to evaluate the stability of the thin films at such a temperature.

Figure 2a−c presents the XRD patterns over time of pristine and treated films at a fixed temperature of 150 °C, in the range 2θ = 12−15°. This allows one to evidence the loss of MAPI (vanishing of the peak at 2θ = 14.0°)[26] and the subsequent rise of PbI$_2$ (rise of the peak at 2θ = 12.6°). In order to have semiquantitative analysis of the degradation, we computed the intensity ratio of MAPI and PbI$_2$ main peaks (2θ = 14.0 and 12.6°), which is proportional to the relative amount of both species in the sample. This ratio is plotted in Figure 2d. The initial MAPI/PbI$_2$ ratio is not infinite because from the very first scan a slight contribution from PbI$_2$ is already observed. This is very common in perovskite films and can be due either to impurities during the synthesis/deposition or even to a slight degradation already occurring during exposure of the samples to air prior to the first analysis. In any case, the initial fraction of PbI$_2$ is low, as can be seen from Figure 2. This fraction

increases over time for all samples, though not at the same pace. Indeed, treated samples are significantly more stable.

As an arbitrary measure, we may consider the time t_{10} by which the PbI_2 peak has reached an intensity equal to 10% of the main perovskite peak. As can be seen in Figure 2d, t_{10} goes from less than 2 h for pristine MAPI to 4 h for TOPO-treated films and to 8 h for TDMAI-treated ones. This reveals that coated MAPI films can withstand high temperature much better than pristine ones. In other terms, surface coating with organic molecules allows the film to be processed at temperatures above 100 °C for longer times, during which the deposition of further materials or hot encapsulation of devices can take place. This stability test at high temperature can also be seen as an accelerated test of the degradation that occurs already at room temperature. Indeed, at room temperature, pristine films were found to be quickly degraded ($t_{10} < 2$ weeks), while coated ones were not significantly altered even after 3 weeks (see Figure S2). These results suggest a combined contribution from the coating molecule's head group and alkyl chains to the enhanced stability of the film. Indeed, as previously suggested by others,[21] the hydrophobic nature of the alkyl chains present on both TDMAI and TOPO may block moisture-derived degradation. However, the fact that TDMAI-coated samples are more stable than TOPO-coated ones suggests that the higher affinity of the MAI head group (which can perfectly fit in the MAPI structure) in contrast with the P═O group of TOPO (which is not known to specifically bind to MAPI) may also play an important role. More detailed investigations on these fundamental aspects are however needed to draw unambiguous conclusions.

We fabricated different solar cells with pristine and treated MAPI. Although TDMAI yielded the highest material stability (Figure 2), we were not able to fabricate efficient and reproducible devices with it. Two reasons may explain this evidence: either the TDMAI layer was too thick (which would also explain the highest stability) and did not allow charge transfer in the device or the process induced other negative consequences in the film such as the occurrence of pinholes that lead to short circuits. The first hypothesis is not in accordance with our XPS analysis, which reveals a strong signal for lead (Figure 1a) and suggests that the MAPI film is not covered by a thick (>5 nm) uniform insulating layer. On the other hand, because the coating process, adapted from Yang et al.,[21] is based on full immersion of the film in a fairly polar solvent (isopropanol), which might partially degrade the perovskite, the second hypothesis seems more plausible.

In contrast, we were able to fabricate solar cells with TOPO-coated MAPI films. Indeed, although TOPO is insulating, charge extraction by tunneling through an insulating layer can be achieved if the layer is thin enough, as also observed by others.[24,27] The TOPO layer thickness can be estimated by the intensity drop of I 3d and Pb 4f XPS peaks (see Figure S3). Indeed, as MAPI is covered by an organic layer, photoelectrons from the underlying lead and iodine atoms will be absorbed following Beer–Lambert law. Hence, the intensity of the peaks (or rather peak areas) will decrease as follows: $A_{TOPO}(X) = A_{Pristine}(X)e^{-\lambda/d}$, where $A_{TOPO}(X)$ and $A_{Pristine}(X)$ are the area corresponding to XPS peak X (in this case I 3d and Pb 4f) in the presence or absence of TOPO, λ is the inelastic mean free path of photoelectrons in the TOPO layer, and d is the thickness of the layer. If we assume $\lambda = 3$ nm as a common value for organic material,[28] then we obtain $d = \lambda \times \ln(A_{Pristine}(I\ 3d)/A_{TOPO}(I\ 3d)) = 0.5$ nm (considering iodine peaks) or $d = \lambda \times \ln(A_{Pristine}(Pb\ 4f)/A_{TOPO}(Pb\ 4f)) = 0.6$ nm (considering lead peaks). Both values are close to and consistent with a single monolayer of TOPO. As we will show hereafter, this monolayer of TOPO does not degrade the device performance (Figure 3).
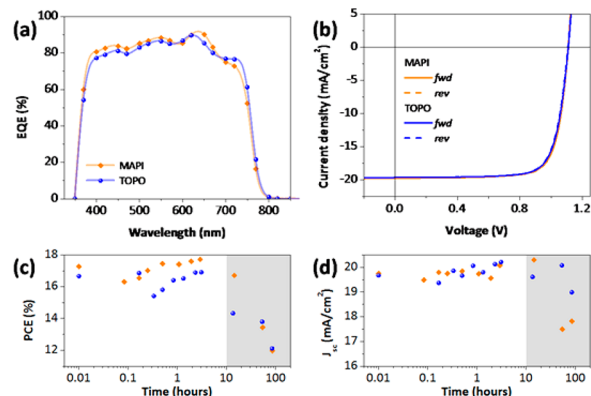

Figure 3. (a) EQE spectra and (b) J−V curves under illumination for solar cells with pristine MAPI (orange squares) and MAPI functionalized with TOPO (blue spheres). (c) Efficiency and (d) photocurrent of the same cells recorded over time during air exposure and without any encapsulation. See Figure S5 for more statistics on TOPO samples.

In contrast, when a more concentrated solution of TOPO is used, resulting in a slightly thicker layer (see Figure S1), the device performs significantly worse (see Figure S4). This highlights the critical importance of the coating layer thickness. The cells were prepared with vacuum-deposited MAPI in the n−i−p configuration, avoiding the use of doped transport layers in order to be able to test their stability in air without encapsulation. For this purpose, we coated the indium tin oxide (ITO)/glass substrates with a bilayer of TiO_2 nanoparticles (50 nm) in combination with a thin (10 nm) C60 film in contact with MAPI. The fullerene layer was introduced in order to reduce carrier recombination at the TiO_2 electron transport layer.[13] After deposition of the perovskite, a double hole transport layer composed of N4,N4,N4″,N4″-tetra([1,1′-biphenyl]-4-yl)-[1,1′:4′,1″-terphenyl]-4,4″-diamine (TaTm, 10 nm) and MoO_3 (10 nm) was sublimated onto the MAPI, and the device was finished with a gold electrode (100 nm). Figure 3a shows the external quantum efficiency (EQE) spectra for solar cells with and without the TOPO layer. Their spectral response was fairly similar (small differences are due to batch-to-batch variations) and above 80% over all of the visible spectrum. This resulted in a short-circuit current density of 19.7 mA/cm^2 for both devices. The current density versus voltage (J−V) curves recorded under 1 sun illumination (Figure 3b) were practically identical in the presence of TOPO, suggesting that charge transport and recombination are substantially unaltered by its presence. Also, the J−V curves recorded in forward (fwd) and reverse (rev) are virtually hysteresis-free. The open-circuit voltage (V_{oc}) was as high as 1100 mV, and we noted only a small reduction in the fill factor (from 78.8 to 77.1%) upon TOPO treatment. The resulting power conversion efficiency (PCE) was 17.2% for the solar cell using pristine MAPI and 16.7% for the one with TOPO-modified perovskite.

We tested the stability of the cells in air without any encapsulation, measuring the J−V curves over time. We observed a first drop in the efficiency followed by a slow

recovery during the first 10 h (Figure 3c), after which the device performance started to drop. While the PCE of the devices decreased in a similar manner independently of the use of the TOPO layer, we observed how the cells with TOPO-modified MAPI retained the photocurrent for a much longer time (Figure 3d), with a slower decrease as compared to the pristine MAPI cells. As the photocurrent is mainly determined by the rate of carrier generation within the perovskite, this might indicate that the presence of TOPO can alleviate the perovskite degradation when incorporated in a working device, in analogy with the results presented for simple perovskite films (Figure 2).

In summary, we have shown that surface coating with organic molecules can greatly enhance the stability of pure MAPI thin films at high temperature, as well as room temperature. This methodology is promising for enhancing both the processability window of the material and the long-term operational stability. Indeed, we have shown that efficient solar cells could be fabricated with functionalized MAPI thin films. While the photocurrent was observed to be maintained for a longer time during air exposure of the cells, further developments, optimizing the choice of organic molecules and the deposition method, should allow one to enhance the stability while minimizing efficiency losses. Furthermore, a deeper study on halide perovskite surface functionalization would certainly shed more light on the binding mechanisms of different molecules on perovskites.

■ ASSOCIATED CONTENT

ⓢ Supporting Information

The Supporting Information is available free of charge on the ACS Publications website at DOI: 10.1021/acsenergy-lett.8b00193.

Experimental details, XPS of samples with different amounts of TOPO, XRD of samples aged at room temperature, and J–V curves of devices based on different amounts of TOPO (PDF)

■ AUTHOR INFORMATION

Corresponding Author

*E-mail: Francisco.palazon@uv.es.

ORCID 🟢

Francisco Palazon: 0000-0002-1503-5965

Mirko Prato: 0000-0002-2188-8059

Michele Sessolo: 0000-0002-9189-3005

Henk J. Bolink: 0000-0001-9784-6253

Liberato Manna: 0000-0003-4386-7985

Notes

The authors declare no competing financial interest.

■ ACKNOWLEDGMENTS

■ REFERENCES

(1) Stranks, S. D.; Snaith, H. J. Metal-Halide Perovskites for Photovoltaic and Light-Emitting Devices. *Nat. Nanotechnol.* **2015**, *10* (5), 391−402.

(2) Zhao, Y.; Zhu, K. Organic−inorganic Hybrid Lead Halide Perovskites for Optoelectronic and Electronic Applications. *Chem. Soc. Rev.* **2016**, *45* (3), 655−689.

(3) Sutherland, B. R.; Sargent, E. H. Perovskite Photonic Sources. *Nat. Photonics* **2016**, *10* (5), 295−302.

(4) Kim, Y.-H.; Cho, H.; Lee, T.-W. Metal Halide Perovskite Light Emitters. *Proc. Natl. Acad. Sci. U. S. A.* **2016**, *113* (42), 11694−11702.

(5) Stranks, S. D.; Stranks, S. D.; Eperon, G. E.; Grancini, G.; Menelaou, C.; Alcocer, M. J. P.; Leijtens, T.; Herz, L. M.; Petrozza, A.; Snaith, H. J.; et al. Electron-Hole Diffusion Lengths Exceeding 1 Micrometer in an Organometal Trihalide Perovskite Absorber. *Science* **2013**, *342* (6156), 341−344.

(6) De Wolf, S.; Holovsky, J.; Moon, S.-J.; Löper, P.; Niesen, B.; Ledinsky, M.; Haug, F.; Yum, J.; Ballif, C. Organometallic Halide Perovskites: Sharp Optical Absorption Edge and Its Relation to Photovoltaic Performance. *J. Phys. Chem. Lett.* **2014**, *5*, 1035−1039.

(7) Petrus, M. L.; Schlipf, J.; Li, C.; Gujar, T. P.; Giesbrecht, N.; Müller-Buschbaum, P.; Thelakkat, M.; Bein, T.; Hüttner, S.; Docampo, P. Capturing the Sun: A Review of the Challenges and Perspectives of Perovskite Solar Cells. *Adv. Energy Mater.* **2017**, *7* (16), 1−27.

(8) Manser, J. S.; Saidaminov, M. I.; Christians, J. A.; Bakr, O. M.; Kamat, P. V. Making and Breaking of Lead Halide Perovskites. *Acc. Chem. Res.* **2016**, *49* (2), 330−338.

(9) Leijtens, T.; Bush, K.; Cheacharoen, R.; Beal, R.; Bowring, A.; McGehee, M. D. Towards Enabling Stable Lead Halide Perovskite Solar Cells; Interplay between Structural, Environmental, and Thermal Stability. *J. Mater. Chem. A* **2017**, *5* (23), 11483−11500.

(10) Rehman, W.; McMeekin, D. P.; Patel, J. B.; Milot, R. L.; Johnston, M. B.; Snaith, H. J.; Herz, L. M. Photovoltaic Mixed-Cation Lead Mixed-Halide Perovskites: Links between Crystallinity, Photo-Stability and Electronic Properties. *Energy Environ. Sci.* **2017**, *10* (1), 361−369.

(11) Kubicki, D. J.; Prochowicz, D.; Hofstetter, A.; Zakeeruddin, S. M.; Grätzel, M.; Emsley, L. Phase Segregation in Cs-, Rb- and K-Doped Mixed-Cation (MA)x(FA)1-xPbI3Hybrid Perovskites from Solid-State NMR. *J. Am. Chem. Soc.* **2017**, *139* (40), 14173−14180.

(12) Zhang, M.; Yun, J. S.; Ma, Q.; Zheng, J.; Lau, C. F. J.; Deng, X.; Kim, J.; Kim, D.; Seidel, J.; Green, M. A.; et al. High-Efficiency Rubidium-Incorporated Perovskite Solar Cells by Gas Quenching. *ACS Energy Lett.* **2017**, *2* (2), 438−444.

(13) Forgács, D.; Pérez-del-Rey, D.; Ávila, J.; Momblona, C.; Gil-Escrig, L.; Dänekamp, B.; Sessolo, M.; Bolink, H. J. Efficient Wide Band Gap Double Cation − Double Halide Perovskite Solar Cells. *J. Mater. Chem. A* **2017**, *5* (7), 3203−3207.

(14) Grancini, G.; Roldán-Carmona, C.; Zimmermann, I.; Mosconi, E.; Lee, X.; Martineau, D.; Narbey, S.; Oswald, F.; De Angelis, F.; Graetzel, M.; et al. One-Year Stable Perovskite Solar Cells by 2D/3D Interface Engineering. *Nat. Commun.* **2017**, *8*, 15684.

(15) Tsai, H.; Nie, W.; Blancon, J. C.; Stoumpos, C. C.; Asadpour, R.; Harutyunyan, B.; Neukirch, A. J.; Verduzco, R.; Crochet, J. J.; Tretiak, S.; et al. High-Efficiency Two-Dimensional Ruddlesden-Popper Perovskite Solar Cells. *Nature* **2016**, *536* (7616), 312−317.

(16) Smith, I. C.; Hoke, E. T.; Solis-Ibarra, D.; McGehee, M. D.; Karunadasa, H. I. A Layered Hybrid Perovskite Solar-Cell Absorber with Enhanced Moisture Stability. *Angew. Chem., Int. Ed.* **2014**, *53* (42), 11232−11235.

(17) Cao, D. H.; Stoumpos, C. C.; Farha, O. K.; Hupp, J. T.; Kanatzidis, M. G. 2D Homologous Perovskites as Light-Absorbing Materials for Solar Cell Applications. *J. Am. Chem. Soc.* **2015**, *137* (24), 7843−7850.

(18) Lira-Cantú, M. Perovskite Solar Cells: Stability Lies at Interfaces. *Nat. Energy* **2017**, *2*, 17115.

366 (19) Saliba, M.; Matsui, T.; Domanski, K.; Seo, J.-Y.; Ummadisingu,
367 A.; Zakeeruddin, S. M.; Correa-Baena, J.-P.; Tress, W. R.; Abate, A.;
368 Hagfeldt, A.; et al. Incorporation of Rubidium Cations into Perovskite
369 Solar Cells Improves Photovoltaic Performance. *Science (Washington,
370 DC, U. S.)* **2016**, *354*, 206.
371 (20) Wang, Q.; Chen, B.; Liu, Y.; Deng, Y.; Bai, Y.; Dong, Q.; Huang,
372 J. Scaling Behavior of Moisture-Induced Grain Degradation in
373 Polycrystalline Hybrid Perovskite Thin Films. *Energy Environ. Sci.*
374 **2017**, *10* (2), 516−522.
375 (21) Yang, S.; Wang, Y.; Liu, P.; Cheng, Y.-B.; Zhao, H. J.; Yang, H.
376 G. Functionalization of Perovskite Thin Films with Moisture-Tolerant
377 Molecules. *Nat. Energy* **2016**, *1* (2), 15016.
378 (22) Wang, F.; Geng, W.; Zhou, Y.; Fang, H. H.; Tong, C. J.; Loi, M.
379 A.; Liu, L. M.; Zhao, N. Phenylalkylamine Passivation of Organolead
380 Halide Perovskites Enabling High-Efficiency and Air-Stable Photo-
381 voltaic Cells. *Adv. Mater.* **2016**, *28* (45), 9986−9992.
382 (23) Dequilettes, D. W.; Koch, S.; Burke, S.; Paranji, R. K.;
383 Shropshire, A. J.; Ziffer, M. E.; Ginger, D. S. Photoluminescence
384 Lifetimes Exceeding 8 Ms and Quantum Yields Exceeding 30% in
385 Hybrid Perovskite Thin Films by Ligand Passivation. *ACS Energy Lett.*
386 **2016**, *1* (2), 438−444.
387 (24) Huang, G.; Wang, C.; Zhang, H.; Xu, S.; Xu, Q.; Cui, Y. Post-
388 Healing of Defects: An Alternative Way for Passivation of Carbon-
389 Based Mesoscopic Perovskite Solar Cells *via* Hydrophobic Ligand
390 Coordination. *J. Mater. Chem. A* **2018**, *6* (6), 2449−2455.
391 (25) Momblona, C.; Gil-Escrig, L.; Bandiello, E.; Hutter, E. M.;
392 Sessolo, M.; Lederer, K.; Blochwitz-Nimoth, J.; Bolink, H. J. Efficient
393 Vacuum Deposited P-I-N and N-I-P Perovskite Solar Cells Employing
394 Doped Charge Transport Layers. *Energy Environ. Sci.* **2016**, *9* (11),
395 3456−3463.
396 (26) Shao, F.; Xu, L.; Tian, Z.; Xie, Y.; Wang, Y.; Sheng, P.; Wang,
397 D.; Huang, F. A Modified Two-Step Sequential Deposition Method
398 for Preparing Perovskite $CH_3NH_3PbI_3$ Solar Cells. *RSC Adv.* **2016**,
399 *6* (48), 42377−42381.
400 (27) Lee, W. H.; Chen, C. Y.; Li, C. S.; Hsiao, S. Y.; Tsai, W. L.;
401 Huang, M. J.; Cheng, C. H.; Wu, C. I.; Lin, H. W. Boosting Thin-Film
402 Perovskite Solar Cell Efficiency through Vacuum-Deposited Sub-
403 Nanometer Small-Molecule Electron Interfacial Layers. *Nano Energy*
404 **2017**, *38*, 66−71.
405 (28) Tanuma, S.; Powell, C. J.; Penn, D. R. Calculations of Electron
406 Inelastic Mean Free Paths. V. Data for 14 Organic Compounds over
407 the 50−2000 eV Range. *Surf. Interface Anal.* **1994**, *21* (3), 165−176.